Predicting the Onset of the North Australian Wet Season with the POAMA Dynamical Prediction System

WASYL DROSDOWSKY AND MATTHEW C. WHEELER

Centre for Australian Weather and Climate Research, Bureau of Meteorology, Melbourne, Victoria, Australia

(Manuscript received 24 July 2013, in final form 17 October 2013)

ABSTRACT

A forecast product focusing on the onset of the north Australian wet season using a dynamical ocean–atmosphere model is developed and verified. Onset is defined to occur when a threshold rainfall accumulation of 50 mm is reached from 1 September. This amount has been shown to be useful for agricultural applications, as it is about what is required to generate new plant growth after the usually dry period of June–August. The normal (median) onset date occurs first around Darwin in the north and Cairns in the east in late October, and is progressively later for locations farther inland away from these locations. However, there is significant interannual variability in the onset, and skillful predictions of this can be valuable. The potential of the Predictive Ocean–Atmosphere Model for Australia (POAMA), version 2, for making probabilistic predictions of onset, derived from its multimember ensemble, is shown. Using 50 yr of hindcasts, POAMA is found to skillfully predict the variability of onset, despite a generally dry bias, with the ''percent correct'' exceeding 70% over about a third of the Northern Territory. In comparison to a previously developed statistical method based solely on El Niño–Southern Oscillation, the POAMA system shows improved skill scores, suggesting that it gains from additional sources of predictability. However, the POAMA hindcasts do not reproduce the observed long-term trend in onset dates over inland regions to an earlier date despite being initialized with the observed warming ocean temperatures. Understanding and modeling this trend should lead to further enhancements in skill.

1. Introduction

Seasonal climate outlooks issued by the National Climate Centre of the Australian Bureau of Meteorology currently consist of probabilistic forecasts of total seasonal rainfall. For some agricultural applications, the timing of rainfall, and especially the relative (to normal) timing of a sharp transition from dry to wet conditions (or vice versa), can be more useful.

Northern Australia is often described as having a monsoon climate. However, if a distinction is made between the monsoon, characterized by a large-scale circulation regime change from easterly to westerly winds (Drosdowsky 1996), and the wet season, defined as the period of rains after the dry season (Nicholls et al. 1982), then only the relatively small area over the Top End and northern Cape York Peninsula actually experiences a classic monsoon in most years (Fig. 5.1 in Wheeler and McBride 2011), while a much larger region comprising most of northern Australia experiences a pronounced wet and dry season (Nicholls 1984). Even in those areas with a classic monsoon wind reversal, a substantial portion of the wet season rainfall is usually received before the large-scale circulation regime change (Nicholls et al. 1982). Concentrating on wet season onset is therefore of greater application value to a larger portion of Australia, and is also often a more agriculturally significant parameter.

Various wet season onset definitions have been proposed for northern Australia. Lo et al. (2007) provide an overview and chose to concentrate on one of the simplest, namely the date of accumulation of 50 mm of rainfall starting from 1 September. This amount was argued to be useful for agricultural applications, as this is about the amount of rainfall that is required to generate new plant growth after the usually dry July–August period (Cook and Heerdegen 2001), and onset defined this way was found to be well related to the ecological green season dates of McCown (1981).

Corresponding author address: Dr. Matthew C. Wheeler, CAWCR, Bureau of Meteorology, GPO Box 1289, Melbourne, VIC 3001, Australia.
E-mail: m.wheeler@bom.gov.au

DOI: 10.1175/WAF-D-13-00091.1

We thus use the same definition in this study. Typical dates for this onset range from late October to late February.

Given the applicability and usefulness of wet season onset, several papers have investigated the prediction of its interannual variability, and its relationship to El Niño–Southern Oscillation (ENSO) has been well described (Nicholls et al. 1982; Nicholls 1984; Lo et al. 2007). In the most recent of these, Lo et al. (2007) developed a statistical prediction system for the probability of an early or late onset (relative to the climatological average) using the antecedent July–August Southern Oscillation index (SOI) as the predictor, showing useful skill. Here, we examine the long-range prediction of onset at lead times of up to 3 months using the Predictive Ocean–Atmosphere Model for Australia (POAMA), the Bureau of Meteorology's coupled prediction system. As we show below, we are able to achieve greater prediction skill than the statistical method of Lo et al. (2007).

2. Data and modeling method

a. Observational data

The observational rainfall data used are from the Australian Water Availability Project (AWAP, Jones et al. 2009). The daily AWAP analyses cover the Australian continent at 0.05° resolution, and are available from 1900, although we only use data from 1960 in this study at a reduced spatial resolution of 1°. The regridding is performed by averaging all 0.05° gridpoint data within each 1° square, matching the same resolution as used by Lo et al. (2007). Observed onset dates are calculated over a spatial subset north of 28°S, and over the period of available hindcasts from POAMA (see below). We exclude grid boxes that have an insufficient number of observing sites such as over parts of central Australia.

b. POAMA system

The POAMA system is in a state of constant development and refinement. The first operational version (POAMA 1.5) ran until November 2011. The current (as of 2013) operational version is POAMA 2, for which there is both a seasonal (P2-S) and newer multiweek (P2-M) forecast stream. A detailed description of these different versions and a comparison of their general skill levels can be found in Hudson et al. (2013). Here, we use both P2-S and P2-M, with the main differences between them being in their procedure for producing an ensemble of initial states, the frequency with which their hindcasts and real-time forecasts are run, and in the number of years of hindcasts (see below for more details).

The atmospheric component of P2-S and P2-M is the Bureau of Meteorology Atmospheric Model (BAM3.0) with T47 horizontal resolution and 17 vertical levels. The ocean component is the Australian Community Ocean Model (ACOM2) with a zonal resolution of 2°, a meridional resolution of 0.5° in the tropics gradually increasing to 1.5° near the poles, and 25 vertical levels. To provide some estimate of model uncertainty, three different configurations of the base model are used for both P2-S and P2-M. The three configurations are differentiated by their use of (a) modified atmospheric physics in the form of an alternative shallow convection parameterization, (b) bias correction of fluxes at the air–sea interface, and (c) no bias correction and standard atmospheric physics. We will refer to these using the letters a, b, and c. By combining results from each configuration (see more below), a simple multimodel ensemble can be computed.

The procedures for computing an ensemble of initial conditions are quite different between P2-S and P2-M. For P2-S, the same atmospheric state is used for each ensemble member, with 10 perturbed ocean states. For P2-M, which is aimed at providing forecasts at shorter lead times, a fully coupled atmosphere–ocean scheme is used to generate 11 different initial states that are perturbed in both the ocean and atmosphere. For both P2-S and P2-M, these initial conditions are input into each of the three model configurations (a, b, and c above), providing a total of 30 members for P2-S and 33 members for P2-M. The expectation is that the P2-M ensemble should generally perform better in the first few weeks to months of the forecast, but that it should be much the same as P2-S beyond a month or so (Hudson et al. 2013).

Hindcasts for P2-S are initialized on the first of each month for the period 1960–2010, with real-time forecasts on the 1st and 15th of each month from September 2010. Hindcasts and forecasts are run out to 270 days (approximately 9 months). For hindcasts initialized on 1 September, the latest possible onset date is therefore 270 days or approximately the end of May, while for hindcasts initialized on 1 June the latest possible onset is at the end of February. The forecast start date of 1 June is the earliest considered in this study.

Hindcasts for P2-M are initialized on the 1st, 11th, and 21st of each month for the period 1981–2011, and its hindcasts have also recently been run out to 270 days.

All computations and display of the POAMA data in this study are made on the horizontal output grid of the atmospheric model with approximately 2.5° resolution. For verification, however, the model and observed (verifying) data must be on the same grid. In this work we remap the model hindcast (and forecast) data onto

the finer 1° grid of the observed rainfall data. This is done partly because the model data are a continuous field over the domain of interest, whereas the observed data are noncontinuous, being restricted to land and to those areas with sufficient observing sites, so interpolation of the model data involves less potential for error. Further, verification on the 1° grid also allows for direct comparison with the results of Lo et al. (2007). The remapping is performed using bilinear interpolation. All contour maps presented in this paper have had a 1–2–1 spatial smoother applied at the time of plotting.

3. Observed onset

As described in the introduction, onset for each year at each location is defined as the date on which 50 mm of rainfall is accumulated from 1 September. We also define the typical or normal onset date as the median of the onset dates computed from the individual years (Fig. 1a). Importantly, in some of the drier locations, the threshold for onset may not be reached by the end of the summer season (i.e., by the end of February) in some years. We assign those cases as being a special ''no onset'' value but still include them in the calculation of the median to counterbalance the years of early onset. In Fig. 1a we therefore do not compute or show the median onset for locations that have 50% or more years with no onset, which occurs in the far west of Australia. The other areas of missing data are either over ocean or where there are insufficient observations.

The observed normal onset date by this definition (Fig. 1a) first occurs in the last third of October in three different locations: near Darwin in the north, on the northeast Queensland coast between Cairns and Townsville, and over southeast Queensland. The concept of an onset is less applicable in the last of these locations because there is no real dry season there, with rainfall occurring along the southeast Queensland coast throughout the winter (i.e., July–August) season. The median onset is progressively later farther inland away from these locations, generally occurring after 1 December for locations south and west of 18°S and 145°E, respectively. Over a large part of the region, median onset occurs during the period encompassing the last third of November and the first third of December. These median dates (computed over 1960/61–2009/10) are very similar to the ''trimmed'' mean dates shown by Lo et al. (2007) for 1948/49–2004/05. Where they differ, the Lo et al. (2007) dates tend to be a little later, but by no more than 10 days. This difference can mostly be explained by the long-term trend (see below).

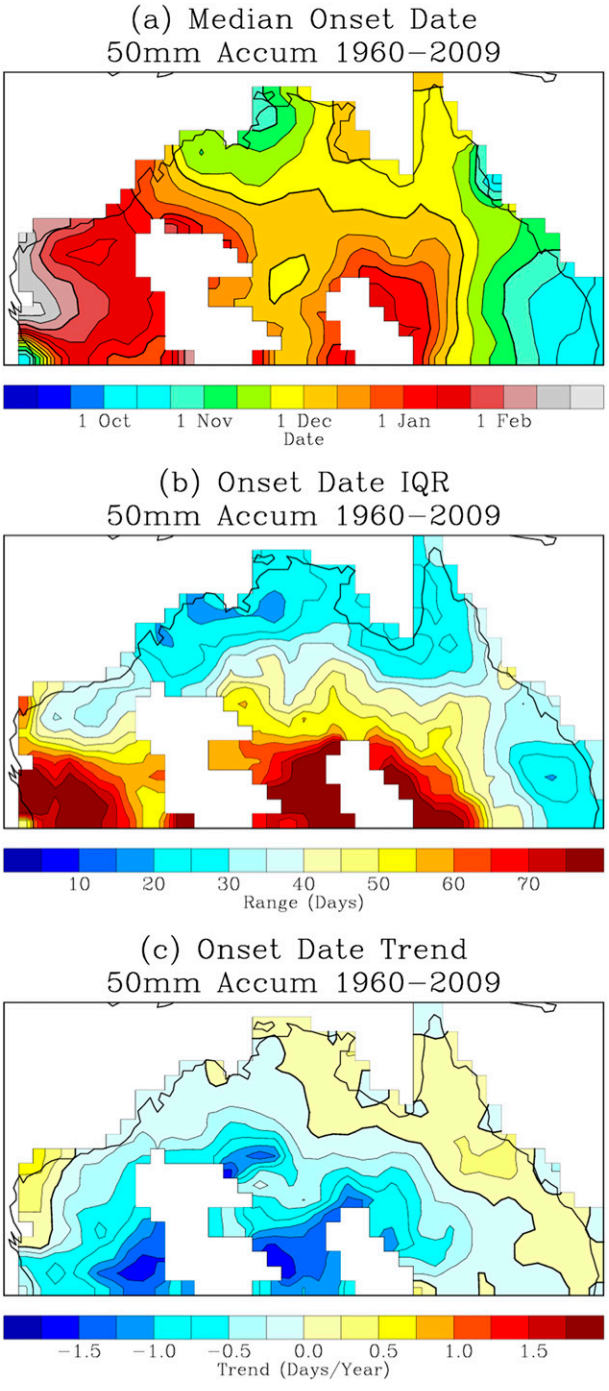

FIG. 1. Observed (a) median, (b) interquartile range (range between the 25th and 75th percentiles), and (c) linear trend of wet season onset dates from 1960/61 to 2009/10. Oceans, and land regions with *no onset* in 50% or more years, are masked out. In (a) the contour lines are drawn at the 1st, 11th, and 21st of each month with a thicker line for the 1st. A 1–2–1 spatial smoothing is applied to all contour maps in this paper at the time of plotting.

The interannual variability in the onset dates, as defined by the interquartile range (i.e., the difference between the 75th and 25th percentiles; Fig. 1b), is lowest in the same areas as the earliest median onset, such as near Darwin and along the east coast, and highest over the inland areas. Much of the interannual variability is due to ENSO, as evident in conditional median onset dates for years of high (>8.0) and low (<−8.0) July–August SOI (Fig. 2). This strong dependence on ENSO was the basis for the statistical forecast schemes of Nicholls (1984) and Lo et al. (2007), and should provide skill using POAMA since it has a demonstrated skill in predicting both ENSO (Hudson et al. 2011) and its associated rainfall anomalies over northern Australia in austral spring (Cottrill et al. 2013).

Rainfall over Australia has shown major trends over the past 50 yr (Nicholls and Collins 2006). In northern Australia there has been an increase in summer (i.e., December–February) rainfall over most of the region, especially in the northwest, but little change in spring. In terms of onset date, these rainfall trends correspond to a strong trend (of over 50 days in 50 yr; Fig. 1c) toward earlier onset over the southern inland regions (of northern Australia) where mean onset typically occurs during December and January, but a much weaker trend over the far north where onset typically occurs earlier. In central Australia near Alice Springs the trend has been $-1.5\,\text{days}\,\text{yr}^{-1}$, or 75 days earlier over the 1960–2009 period. These substantial trends may confound predictions of onset in these regions.

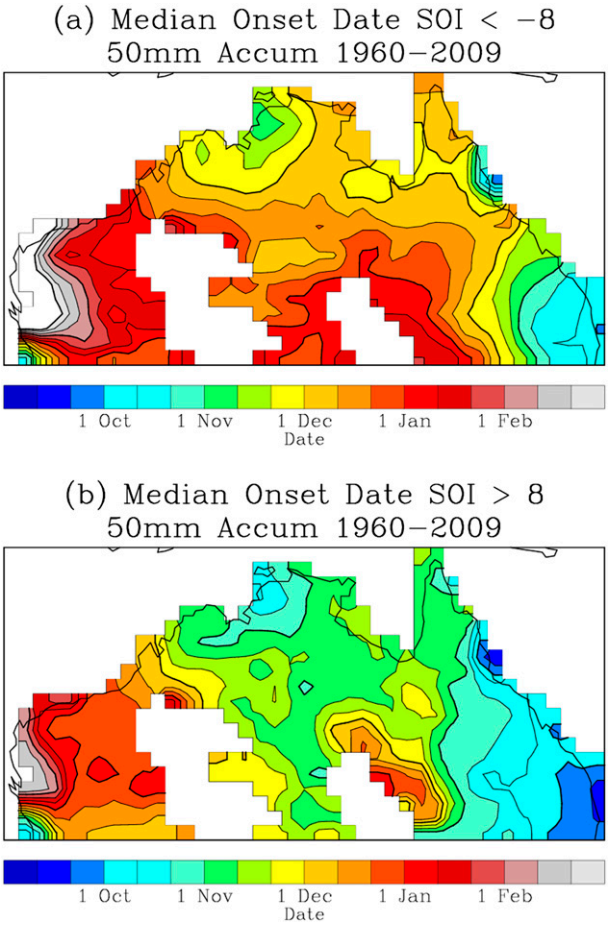

FIG. 2. Observed median wet season onset dates for (a) El Niño years (July–August SOI < −8.0) and (b) La Niña years (SOI > 8.0).

4. POAMA forecasts

In the presentation below we focus initially on P2-S, as this is the version that we used to develop our method given its earlier availability than P2-M. P2-S also has a longer hindcast set (back to 1960), which allows for a better comparison with the observed onset climatology and trend.

a. Median onset dates and trend

For each hindcast or forecast ensemble member the onset date at each grid point is calculated in the same way as for the observed data. A separate climatological median onset date is calculated for each model configuration (i.e., P2-Sa, P2-Sb, and P2-Sc) and for each forecast start (i.e., initialization) date (noting that the onset is still defined from accumulations after 1 September). The potential for model and lead-dependent drift (i.e., bias) (Stockdale 1997) is the reason why a separate climatological median onset date is computed for each forecast start date and model configuration. Lim et al. (2009) showed that the earlier version of POAMA (version 1.5) had a dry bias in austral spring over northern Australia. This is also the case for all configurations of P2-S (and P2-M), from all start dates that we consider. The impact that this has on the model's onset dates is illustrated in Fig. 3a, which shows the median onset date for P2-Sa using the hindcasts from 1 September. Compared to the observed median (Fig. 1a), the dates are almost everywhere later. In particular, they are over a month later in parts of Cape York. Correcting for this model dry/late bias in the resulting prediction product is an important component of this work.

As noted earlier, there is a strong multidecadal trend toward earlier wet season onset over parts of northern Australia. However, none of the P2-S configurations, for any start date, reproduce this trend over their hindcast period. Figure 3b shows the trend in the hindcast onset dates for P2-Sa initialized on 1 September over the period 1960–2009. The trend is much smaller than

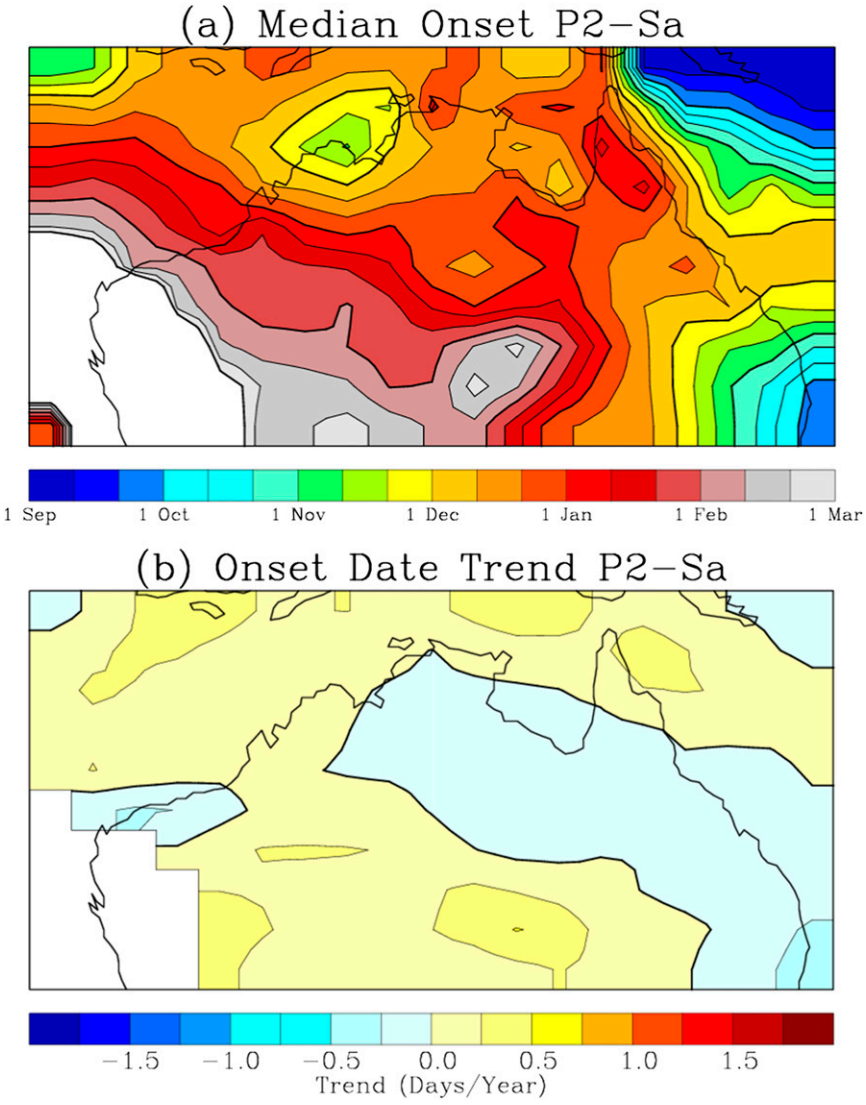

FIG. 3. Modeled (a) median onset date and (b) trend in onset date from P2-Sa hindcasts initialized from 1 September over 1960–2009.

observed (Fig. 1c). Since the model is initialized with global observed sea surface and subsurface ocean temperature observations, this result suggests that the observed rainfall trend is not due to the observed trends in ocean temperatures, such as the strong warming over parts of the Indian Ocean, contrary to the conclusions of Shi et al. (2008) and Lin and Li (2012). However, an alternative explanation is that the model lacks the appropriate summertime rainfall sensitivity to ocean temperatures, consistent with its dry bias. Whatever the reason, we do not attempt to correct for this model shortcoming, although future understanding and modeling of this trend should lead to further enhancements in prediction skill.

b. Correcting for the dry bias

Further demonstration of the characteristics of the dry/late bias is provided in Fig. 4. It shows the cumulative frequency of onset date for the observed data and for the model from its different start dates for one particular configuration (P2-Sa in this case) for a grid point near Darwin. This plot can be interpreted as the cumulative probability that onset has occurred by a certain date. The distribution of onset dates from P2-Sa is similar for all forecast start dates, and if the observed distribution is adjusted by a fixed number of days (38 days later in this case) the shape of the distribution of modeled onset dates is also very similar to

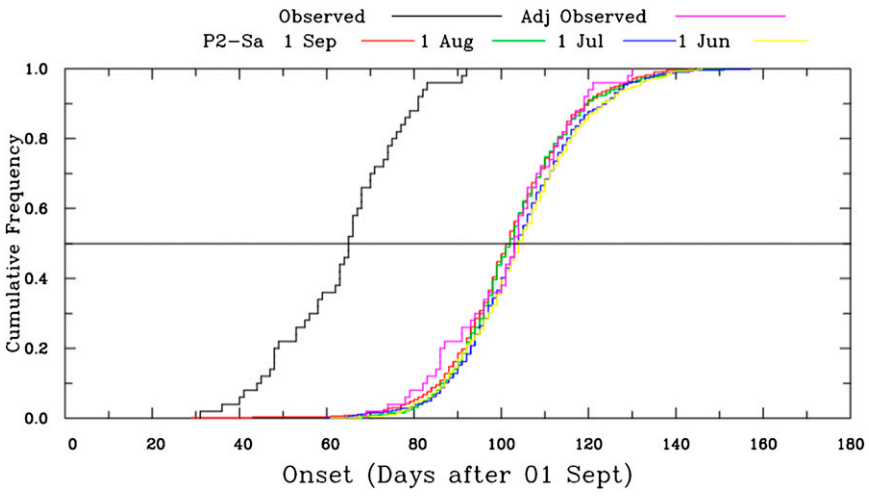

FIG. 4. Cumulative probability of onset occurring by given date, for observations (black) and for P2-Sa from the start dates of 1 Sep (red), 1 Aug (green), 1 Jul (blue), and 1 Jun (yellow), for grid point nearest Darwin. Also shown is the ''adjusted observed'' line, which is the same as the observed except shifted to the right by 38 days.

that observed. That is, the variability of the model onset dates is very similar to the observed, once the fixed adjustment for the dry bias is made. Therefore, it appears adequate to take account of the dry bias by simply computing the forecast onset probabilities (or anomalies), relative to the model onset climatologies, since this method will provide about the same amount of variability about the median as observed. An alternative bias correction procedure we considered was to adjust the required rainfall accumulation amount at each grid point so that the median model onset date matches the median observed date at that point. This process results in very low required accumulation amounts of less than 5 mm in those locations with a pronounced dry bias, especially on Cape York Peninsula. We therefore chose the former method.

c. *Hindcast probabilities*

We concentrate on two different forecast products: the probability of earlier than median onset and the probability of onset in the bottom, middle, and top terciles. We compute the probability of earlier than median onset by counting up the number of ensemble members that have onset occurring before the respective model's climatological median date, and dividing by the total number of members (i.e., 30 members in the case of P2-S). If an ensemble member has its forecast date landing exactly on the median date, then a 50–50 split is given between the early and late categories. We compute the tercile probabilities in a similar way.

Only one spatial map is required to display the probability of early/late onset relative to the median, since there are only two categories and the total probability must add to unity. For the probability of terciles, there are three categories. These can be represented on one spatial map by showing the probability of the highest category at each grid point, although this procedure results in the loss of information regarding the other two categories.

An example hindcast of the probability of earlier than median onset is provided in Fig. 5 for the year 2006. In the left-hand column of Fig. 5 we show the probability of early onset from the hindcasts starting from the three different dates: 1 July, 1 August, and 1 September. From each of these start dates onset was forecast to be more likely late, with increasing confidence (i.e., with probabilities diverging further from 50%) for the successively later start dates. For the latest start date, large areas of central northern Australia were forecast to have less than a 25% chance of earlier than median onset. This verified relatively well, as can be seen by comparing with the verifying observations in the right column of Fig. 5; most of central northern Australia experienced a later than median onset that year. Hindcasts and verifying observations for all years of the P2-S hindcasts are available online (http://poama.bom.gov.au/wet_season/ws_home.shtml).

d. *Hindcast skill: Earlier/later than median*

Three verification measures are used to assess the hindcast performance: the percent correct at each grid point, the Brier skill score (BSS) relative to a climatological forecast at each grid point, and the attributes diagram showing the reliability and resolution of the

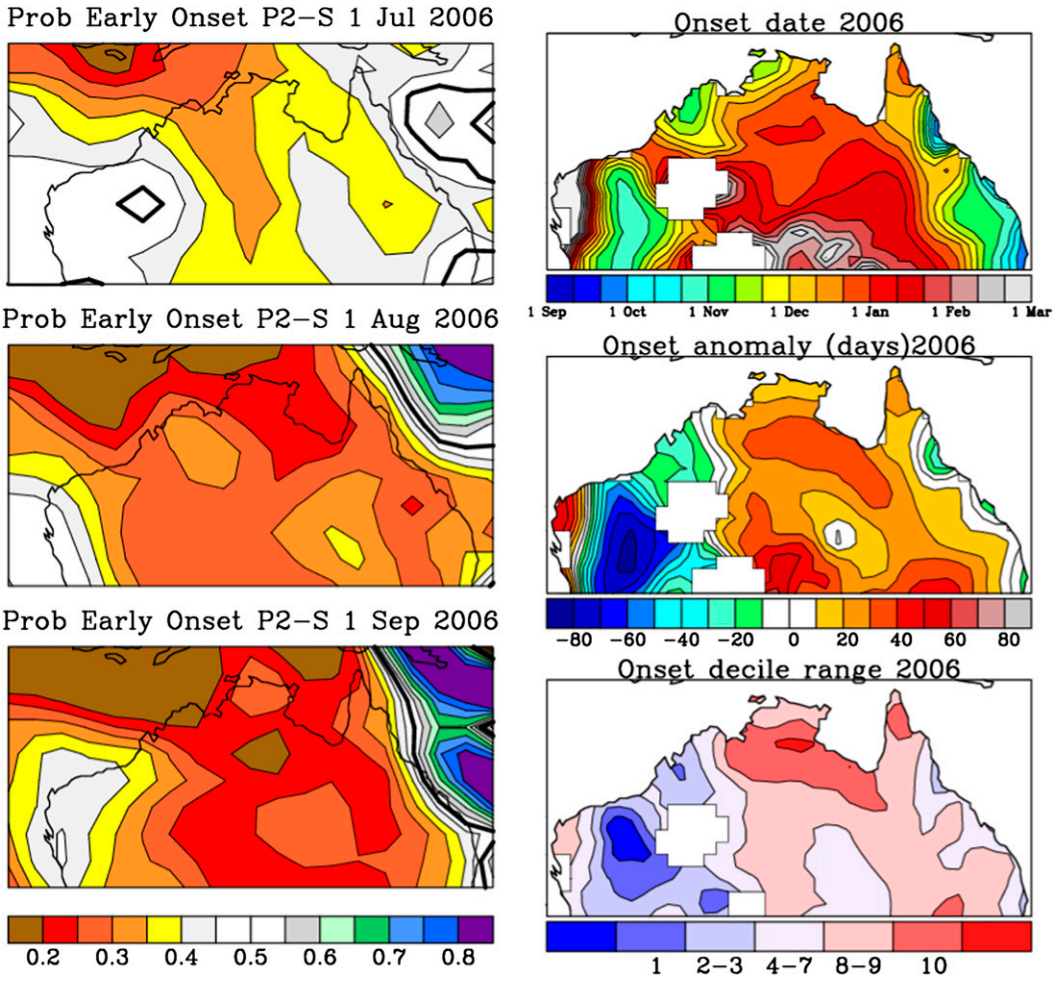

FIG. 5. Hindcast probabilities of early (before median date) wet season onset for the 2006/07 wet season from the hindcast start dates of (bottom left) 1 Sep, (middle left) 1 Aug, and (top left) 1 Jul. Thick contour is for a 50% probability. Shown are (top right) the actual observed onset date and (middle right) onset date as an anomaly, as well as (bottom right) deciles relative to 1960–2009 climatology.

forecasts when pooled over all available grid points north of 28°S. In the left column of Fig. 6 we show these verification measures for P2-S hindcasts of earlier than median onset from the start date of 1 September, and in the right column we show the same for P2-M, which will be discussed later. The P2-S skill plots for the forecasts from July and August are available online (http://poama.bom.gov.au/wet_season/ws_skill.shtml).

For the 1 September start date in P2-S (Fig. 6a), the percent correct exceeds 60% over most of the region and 70% over about a third of the Northern Territory and parts of Queensland, far exceeding the random guess value of 50%. From the earlier forecast start dates (not shown, but see website listed above), the percent correct remains above 60% for most of the domain, although the size of the regions of above 70% are reduced as expected given the longer lead time. The BSS (Fig. 6b) looks similarly encouraging, with up to a 30% improvement over climatology for regions in the Top End and on Cape York Peninsula. The main region of poor skill is in the far southeast corner of the domain. Figure 6b may be compared with Fig. 5a of Lo et al. (2007), noting that the dynamical model (i.e., P2-S) forecast from 1 September provides a very similar lead time to the Lo et al. statistical model using July–August SOI (within a couple of days, the time it takes to run and process POAMA). A comparison shows that the skill from P2-S is at least equal to or higher than the statistical model over most grid points. This is further reflected in area-averaged BSS values (Table 1), which show that the P2-S hindcasts are more skillful for all start dates. In fact, the P2-S forecasts from 1 June have a greater area-averaged BSS (6.86%) than do the Lo

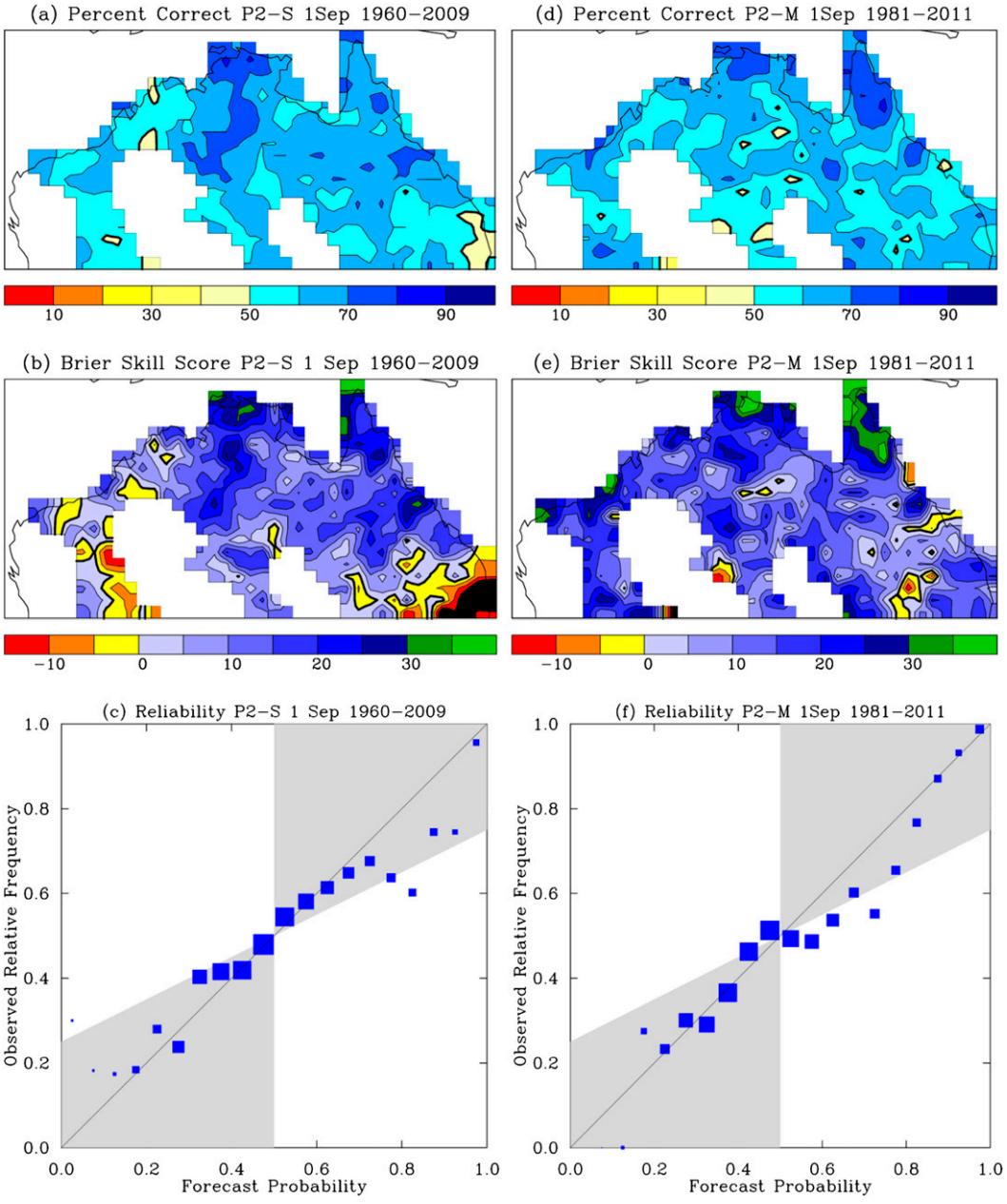

FIG. 6. (left) The verification for P2-S hindcasts initialized on 1 Sep during 1960–2009 for forecasts of early or late onset relative to the median date. (right) The verification for P2-M hindcasts initialized on 1 September during 1981–2011. (a),(d) Percentages correct for probabilistic hindcasts of early or late onset treated as a categorical forecast of most probable category. (b),(e) BSSs as a percentage improvement over a climatological forecast with black shading for a very poor BSS of less than −15%. (c),(f) Reliability or attributes diagrams, pooling all grid points with data north of 28°S. The size (area) of each blue square is proportional to the sample size for each bin of forecasts, and the gray zones show regions where the forecasts contribute positively to the BSS.

et al. results at any lead time (e.g., 5.62% for July–August SOI). The P2-S forecasts also exhibit a high degree of reliability, as shown by the attributes diagram (Fig. 6c). Importantly, the attributes diagram shows that these forecasts do not suffer as much from the overconfidence that is typical of seasonal mean rainfall predictions from POAMA and other seasonal prediction systems, as discussed by Langford and Hendon (2013). We think this may be due to our method for correcting for the dry bias; by computing the probabilities with respect to the much later median onset dates of the model, the effective forecast lead

TABLE 1. Area-averaged BSS (relative to climatology) for POAMA median and tercile hindcasts for forecasts initialized on 1 Sep, 1 Aug, 1 Jul, and 1 Jun. For the tercile hindcasts, the full Brier scores are calculated by summing over all three categories according to the definition of Brier (1950). Comparative skill for the Lo et al. (2007, Table 3) statistical forecasts are also shown (based on hindcasts for 1948–2004). The P2-S skill is based on 50 yr of hindcasts over 1960–2009, and for P2-M is based on the 31 yr covering 1981–2011. All available grid points north of 28°S are averaged.

	1 Sep	1 Aug	1 Jul	1 Jun
Lo et al. (SOI)	5.62	4.29	2.92	
P2-S median	10.85	9.98	10.24	6.86
P2-S tercile	10.86	11.11	10.38	8.78
P2-M median	14.22	10.81	12.73	10.35

time is lengthened, allowing the model ensemble more time to spread.

e. Hindcast skill: Terciles

An example of a tercile probability forecast of onset date is provided in Fig. 7. As described above, we present the tercile probabilities on a single map by only showing the probability of the most likely of the three categories. This map is for the same year (2006) as those displayed for the earlier/later than median forecasts presented in Fig. 5. Like them, the terciles map shows a high chance of a late onset (i.e., onset occurring in the latest tercile) over much of northern Australia, with probabilities as high as 70%–80% for that category.

Verification measures for the tercile forecasts using all hindcasts from the start date of 1 September are presented in Fig. 8. For the percent correct statistic (Fig. 8a), the values need to be compared against a random forecast value of 33.3%. The actual values obtained are over 40% correct for most locations, and over 50% for many locations in the Northern Territory and northeast Queensland. BSS values for the three category tercile forecasts (Fig. 8b) show a similar pattern to the median forecasts (Fig. 6b) but with less extreme values of positive and negative skill, so that the resulting area-averaged BSS is almost identical (Table 1). This good skill is further supported by the attributes diagrams for the earliest (Fig. 8c) and latest (Fig. 8d) terciles. Note that these are computed by considering forecasts of early or late onset against the combination of the other two categories. The diagrams show that the tercile hindcasts also exhibit a high degree of reliability.

f. Forecasts with POAMA-2 multiweek (P2-M)

As already described, P2-M is a newer version of POAMA that was developed to improve multiweek (i.e., weeks to 1 month) performance. Indeed, this version has shown improved skill on this range, but it has also shown improvements on the seasonal time scale (Hudson et al. 2013). Using the same techniques as described above for P2-S, although for the shorter hindcast period of 1981–2011, we have tested the hindcast skill of P2-M for the probabilistic predictions (using all 33 members) of wet season onset with the results presented in the right column of Fig. 6 and the bottom row of Table 1.

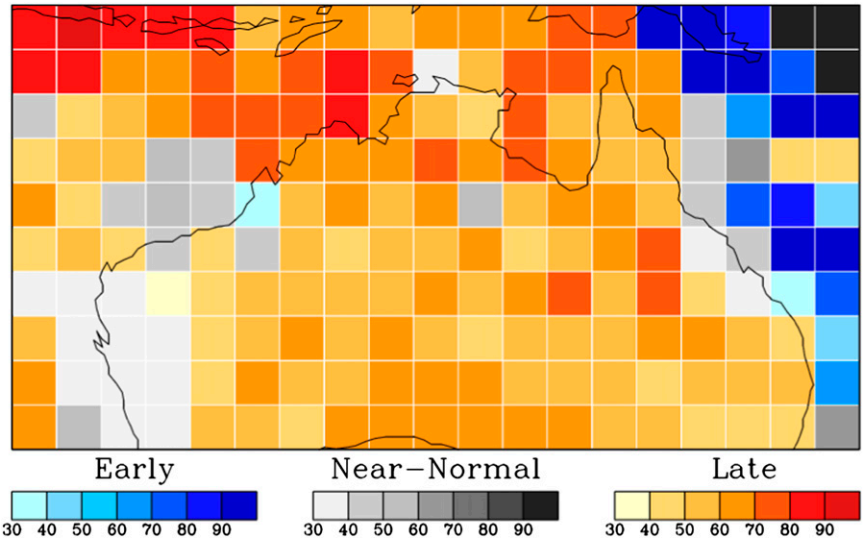

FIG. 7. P2-S hindcast probabilities of most likely tercile category (i.e., early, near normal, or late) for wet season onset during the 2006/07 wet season, from the forecast start date of 1 Sep.

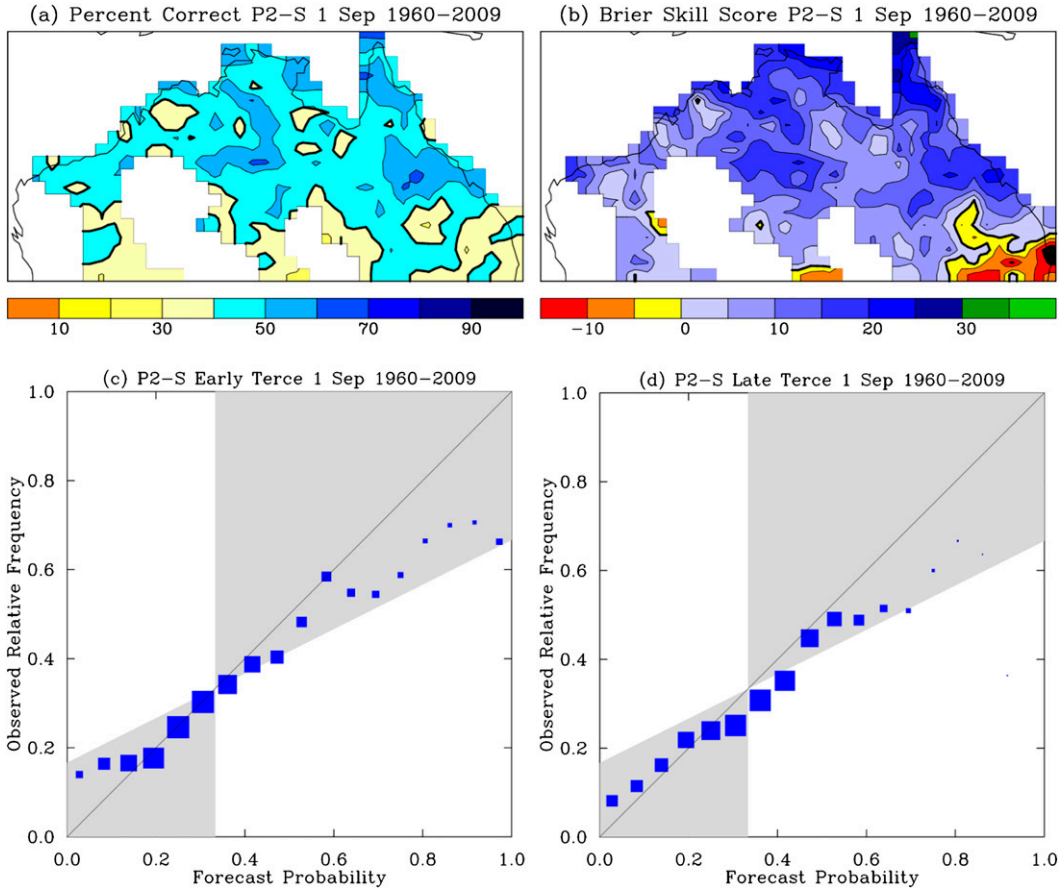

FIG. 8. As in the left column of Fig. 6, but for the tercile probability hindcasts from P2-S. The two separate attributes diagrams are for hindcasts of onset in the (c) bottom (i.e., early) and (d) top (i.e., late) terciles.

Although the verification maps in Fig. 6 show regions of both increased and decreased hindcast performance, the area-averaged results in Table 1 strongly suggest that the overall skill of P2-M is also improved over P2-S for wet season onset, especially for the shortest lead time (i.e., a start date of 1 September). A comparison of the BSS maps (Figs. 6b and 6e) shows substantial improvements in the far southeast and in the west. Therefore, using the new P2-M instead of P2-S for future real-time forecasts appears preferable.

5. Real-time forecasts

The forecast system as described above for the probability of earlier than median onset was already in place for real-time testing with P2-S during the 2011/12 and 2012/13 wet seasons. Here, we present the real-time forecasts that were made.

a. 2011/12 season

Figure 9 shows the real-time forecast from the 1 September 2011 run of P2-S. Forecasts from the earlier model runs in July and August (see http://poama.bom.gov.au/wet_season/ws_forecasts.shtml) produced broadly similar patterns, with a low probability of early onset over most of northern Australia and a high probability along the northeast coast and in the southwest of the domain. Hindcasts from P2-M (noting that P2-M was

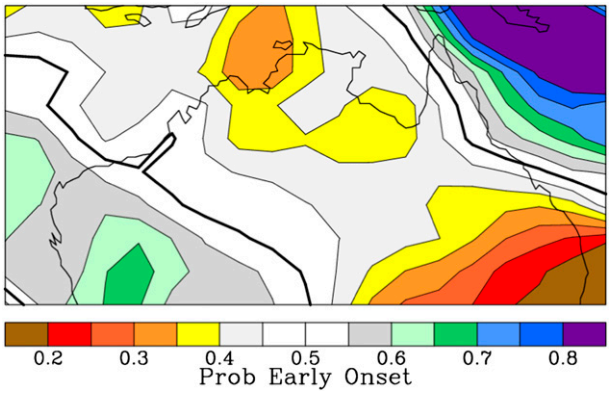

FIG. 9. Probability of early wet season onset for the 2011/12 season, from the real-time forecast initialized on 1 Sep 2011.

not being run in real time in 2011) also show a similar pattern (not shown). Despite the developing weak to moderate 2011/12 La Niña event, which would be expected to cause an early onset, negative sea surface temperature (SST) anomalies were recorded around northern Australia during the July–September period (Cottrill 2012), which was the likely cause of a larger proportion of the model ensemble members forecasting a late onset. Compared to the observed onset, however, these particular forecasts did not verify well. Instead, the actual onset occurred early in the majority of the region, including some small areas of earliest onset on record over the inland regions of Western Australia (not shown). Although it is very difficult to diagnose the reasons for a single forecast failure, we do note that this particular miss is consistent with the long-term trend toward earlier onset in the inland regions (Fig. 1c) that POAMA-2 does not appear to be able to replicate (Fig. 3b).

b. 2012/13 season

For the 2012/13 season, the onset forecasts from P2-S initialized from 1 June and 1 July showed near-neutral probabilities of early onset over northern Australia (see http://poama.bom.gov.au/wet_season/ws_forecasts.shtml), but swung to generally low probabilities of early onset in August and September (Fig. 10). Again, P2-M forecasts (not shown) were similar to the P2-S forecasts. The main climate driver of these forecasts appears to have been the borderline El Niño oceanic conditions observed during July–September 2012. However, after September, conditions in the Pacific and Indian Oceans returned to near neutral and remained at these levels through the austral summer of 2012/13, with the observed onset occurring somewhat early to near normal. We are not too discouraged by this result, however, for the following reasons: 1) it is a probabilistic forecast, so there is always a chance that the less likely outcome will occur; 2) during periods of a weak or variable ENSO state, we know that skill is reduced; and 3) despite a wet to near-normal start to the wet season in the months of September–November, later months were quite dry in many parts of northern Australia.

6. Conclusions

The ability of the latest versions of the POAMA system (P2-S and P2-M) to predict the onset of the wet season over northern Australia, as defined by an accumulation of 50 mm of rainfall from 1 September, has been examined. Fifty years of multimodel ensemble hindcasts from P2-S are analyzed, along with 31 yr from P2-M. The prediction products developed are forecast probabilities of wet season onset being before the median date as well as in the three tercile categories. Special consideration of the generally dry bias of the models is required, for which we compute the forecast probabilities relative to the model's own climatological median and tercile dates, as computed from the hindcasts.

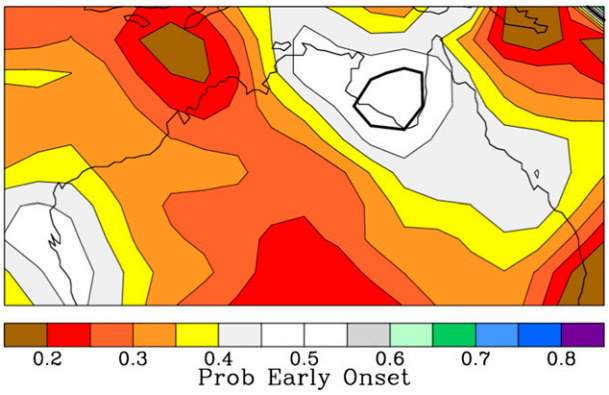

FIG. 10. Probability of early wet season onset for the 2012/13 season, from the real-time forecast initialized on 1 Sep 2012.

Such predictions of wet season onset are a fairly stringent test of the model, since onset can (and often does) occur several months after the start of the accumulation period, and we are also considering lead times of up to 3 months prior to the start of the accumulation period. We are therefore encouraged to see relatively high levels of skill for the hindcasts. Compared to the statistical forecasts of Lo et al. (2007), we compute higher area-averaged BSSs for all equivalent lead times (from the forecast start dates of 1 July, 1 August, and 1 September), with the newer P2-M being the most skillful. This latter result is consistent with that of Hudson et al. (2013), showing that the ensemble generation strategy of P2-M of a perturbed atmosphere, as well as ocean states, provides advantages over the ocean-only perturbation method of P2-S, for at least the first few months of the forecast. The improvement compared to the statistical model, which used only the SOI as a predictor, shows the additional skill that can be derived from a dynamical model that contains a greater range of sources of predictability.

Despite this good news, there are a couple of areas of concern. The first is that the model hindcasts, despite containing aspects of climate change through the use of observationally based ocean initial conditions, do not reproduce the observed multidecadal trend in wet season onset toward earlier dates. The second, which may be related to the first, is that the real-time forecasts of P2-S (and hindcasts of P2-M) during the last two years (2011/12 and 2012/13) have been somewhat disappointing.

Acknowledgments. This work has been supported by the Managing Climate Variability Program managed by the Grains Research and Development Corporation. The Centre for Australian Weather and Climate Research is a partnership between CSIRO and the Bureau of Meteorology. We thank the whole POAMA and related teams (including those in the National Climate Centre) for their dedication to producing and maintaining POAMA, and for supporting its products. In particular, we thank Griffith Young for the POAMA web pages and computing support, Debra Hudson for her scientific expertise, Andrew Watkins and Andy Cottrill for their willingness to make user-friendly products, and Andrew Marshall and Joel Lisonbee for internal reviews.

REFERENCES

Brier, G. W., 1950: Verification of forecasts expressed in terms of probability. *Mon. Wea. Rev.,* **78,** 1–3.

Cook, G. D., and R. G. Heerdegen, 2001: Spatial variations in the duration of the rainy season in monsoonal Australia. *Int. J. Climatol.,* **21,** 1723–1732.

Cottrill, D. A., 2012: Seasonal climate summary Southern Hemisphere (spring 2011): La Niña returns. *Aust. Meteor. Oceanogr. J.,* **62,** 179–192.

——, and Coauthors, 2013: Seasonal forecasting in the Pacific using the coupled model POAMA-2. *Wea. Forecasting,* **28,** 668–680.

Drosdowsky, W., 1996: Variability of the Australian summer monsoon at Darwin: 1957–1992. *J. Climate,* **9,** 85–96.

Hudson, D., O. Alves, H. H. Hendon, and G. Wang, 2011: The impact of atmospheric initialisation on seasonal prediction of tropical Pacific SST. *Climate Dyn.,* **36,** 1155–1171.

——, A. G. Marshall, Y. Yin, O. Alves, and H. H. Hendon, 2013: Improving intraseasonal prediction with a new ensemble generation strategy. *Mon. Wea. Rev.,* **141,** 4429–4449.

Jones, D. A., W. Wang, and R. Fawcett, 2009: High-quality spatial climate data-sets for Australia. *Aust. Meteor. Oceanogr. J.,* **58,** 233–248.

Langford, S., and H. H. Hendon, 2013: Improving reliability of coupled model forecasts of Australian seasonal rainfall. *Mon. Wea. Rev.,* **141,** 728–741.

Lim, E.-P., H. H. Hendon, D. Hudson, G. M. Wang, and O. Alves, 2009: Dynamical forecast of inter–El Niño variations of tropical SST and Australian spring rainfall. *Mon. Wea. Rev.,* **137,** 3796–3810.

Lin, Z., and Y. Li, 2012: Remote influence of the tropical Atlantic on the variability and trend in North West Australia summer rainfall. *J. Climate,* **25,** 2408–2420.

Lo, F., M. C. Wheeler, H. Meinke, and A. Donald, 2007: Probabilistic forecasts of the onset of the north Australian wet season. *Mon. Wea. Rev.,* **135,** 3506–3520.

McCown, R. L., 1981: The climatic potential for beef cattle production in tropical Australia: Part III—Variation in the commencement, cessation and duration of the wet season. *Agric. Syst.,* **7,** 163–178.

Nicholls, N., 1984: A system for predicting the onset of the north Australian wet season. *J. Climatol.,* **4,** 425–435.

——, and D. Collins, 2006: Observed climate change in Australia over the past century. *Energy Environ.,* **17,** 1–12.

——, J. L. McBride, and R. J. Ormerod, 1982: On predicting the onset of the Australian wet season at Darwin. *Mon. Wea. Rev.,* **110,** 14–17.

Shi, G., W. Cai, T. Cowan, J. Ribbe, L. Rotstayn, and M. Dix, 2008: Variability and trend of North West Australia rainfall: Observations and coupled climate modeling. *J. Climate,* **21,** 2938–2959.

Stockdale, T. N., 1997: Coupled ocean–atmosphere forecasts in the presence of climate drift. *Mon. Wea. Rev.,* **125,** 809–818.

Wheeler, M. C., and J. L. McBride, 2011: Australasian monsoon. *Intraseasonal Variability in the Atmosphere–Ocean Climate System,* 2nd ed. W. K. M. Lau and D. E. Waliser, Eds., Springer, 147–198.